ThrustPod: a novel solution for vertical take-off and landing systems

Angelo Lerro[1], Luca Nanu[1] and Piero Gili[1]

[1]Mechanical and Aerospace Engineering Department, Polytechnic of Turin
angelo.lerro@polito.it

Abstract

The work introduces a patented solution, named ThrustPod, to adapt the state-of-the-art fixed-wing aircraft for vertical take-off and landing operations. The proposed system is conceived to overcome the need of tilting surfaces or rotors and to overcome the aerodynamic low performance of multicopters. The ThrustPod is applicable to very light and general aviation aircraft and next generation air vehicles that aim to operate on urban and regional routes. The proposed solution is based on retractable thrusters to provide the required vertical thrust for the take-off and landing phases. The more suitable thrusters can be adopted, e.g. ducted fans or propellers. Another characteristic is the modularity as the ThrustPod can be scaled on different vehicle categories. In fact, the proposed solution can be used on different fixed-wing aircraft to provide vertical and take-off capabilities or to design novel airframes. The work proposes an integrated preliminary design process to optimise both the aircraft and the ThrustPod configuration to define fuselage length, thruster's arrangement, power budget, energy management and performance evaluation of a potential aircraft for urban air mobility applications. The aim of the present work is to present a preliminary design application to evaluate advantages and drawback with respect to the most promising urban air mobility vehicles.

1 Introduction

In the next years is estimated an increase of world population. From the latest prospect from United Nation, [3] the 7.7 billion people in 2019 (around 8 billion at November 2021) will grow up to about 10 billion in 2050: most of the people will live in urban environment and urban growth will increase, leading to higher need in transport development. In addition, climate change is an actual issue from the last century, with an increase of overall global surface temperature, harmful emission contents in the air (like CO_2, N_2O and particulate matters PM2.5 and PM10) and rapid grow in the next years, [4]: a percentage of pollution and temperature rises are due to conventional ground vehicles. Furthermore, the congestion and high population density in large cities leads to a increased amount of time needed for Urban/Sub-urban travels. Noise level in urban environment due to means of transport is a secondary but not less important issue to be reduced [18].

To reduce the above mentioned issues, a class of of aircraft is taking more importance in recent years, the Vertical Take-Off and Landing (VTOL) ones. In [5] different VTOL configurations are shown, with advantages and limitations. The urban air mobility (UAM) is one of the new frontier of the aerospace community. The access to the UAM environment is mainly inspired to full electric aircraft, low noise vehicles, vertical take-off and landing capabilities. All concepts can be grouped in three main categories: 1) multi copters, mainly intended for urban operations and with limited range capability; 2) lift+cruise aircraft, mainly intended for urban and sub-urban operation; 3) aircraft with tilting wing / thrusters, mainly intended for sub-urban and low regional operations. The driving idea behind all different concepts is to optimise two main phases: 1) the hovering, or rotary wing, phase; 2) the cruise, or fixed-wing, phase. Of course, the second phase cannot be applied to multi-copters.

The present work deals with a patented solution intended to split the aforementioned phases in order to be optimised independently. The proposed technology is named ThrustPod (TP) and it is based on retractable thrusters only intended to generate the vertical force for the hovering phases. In fact, the aim is to avoid tilting or rotating surfaces, using smaller ducted propellers that can be retracted inside the pod, or the fuselage itself, during the cruise phase. The proposed solution is able to guarantee a minimum drag and noise for the cruise phases with respect

the lift+cruise aircraft and to reduce the mechanical complexity of tilting thrusters and wing. Moreover, the use of independent thrusters for lift and cruise optimise the design of the propellers that are only required to work around the design point. Therefore, the lack of flap to modify the duct shape or mechanism to modify the propeller pitch are not required. The proposed invention can be a stand alone system useful to convert modern fixed wing aircraft to operate in urban environment or to design a novel electric VTOL (eVTOL) aircraft that integrates the TP. Of course, to convert a modern fixed-wing aircraft requires a partial re-design of the entire aircraft and the TP design is highly dependent on the target aircraft.

The work aims to present an integrated process to design a novel aircraft based on the TP. The proposed trade-off integrates the concurrent preliminary analysis of the drag and mass budgets according to the possible TP configurations. A realistic application is presented.

The work introduces the aircraft system and the patented TP solution overview in 2 and the integrated approach to design possible TP configurations are in 3. Drag and weight estimations are presented in section 4 and 5 respectively. Realistic preliminary design results are presented in 6 before concluding the work.

2 System overview

2.1 Aircraft specifications and mission profile

In this section an overview of the eVTOL aircraft equipped with TP is presented, to better understand its mission and purposes. The main aircraft specifications are:

- Vertical Take-Off and Landing (VTOL): the aircraft shall be able to perform hovering for $4\,\mathrm{min}$, needed for take-off ($60\,\mathrm{s}$), landing ($90\,\mathrm{s}$) and transition phases to/from cruise ($30\,\mathrm{s}$) and emergency operations ($60\,\mathrm{s}$);

- Full electric: the thrust units are powered by electric motors only, in accordance with the environmental, traffic and low noise emissions aircraft missions. A battery storage system is then required depending on motors energy demand;

- Range: the eVTOL aircraft is intended for urban and suburban travel operations. The aircraft shall cover $250\,\mathrm{km}$ in less than $1.5\,\mathrm{h}$;

- Altitude: the aircraft shall be able to carry out the mission taking off from sea level, climb up to $3000\,\mathrm{m}$ (where no pressurisation is required), cruise at $3000\,\mathrm{m}$ and landing at sea level as represented in Figure 1;

- Payload: the aircraft is intended to welcome five (5) passengers (each of $80\,\mathrm{kg}$) along with their own belongings up to $10\,\mathrm{kg}$;

- Flight controls: the aircraft is intended to be flown by one (1) pilot (of $80\,\mathrm{kg}$) along with his own belongings up to $10\,\mathrm{kg}$ with a fly-by-wire flight control system. The control is exploited using aerodynamic surfaces during the fixed-wing phase, whereas the TP thrusters are used to control the hovering phases;

- Dimensions: the aircraft shall not exceed a square whose sides are $8\,\mathrm{m}$ long to allow operations in limited areas (e.g. vertiports);

Along with the latter preliminary operation requirements, other design constraints are added. The wing-tail configuration is a boxed wing in order to introduce a reduction in terms of induced drag and the wing and empennage weights (even if it is not taken into account for conservative reasons).

Considering the preliminary inputs, a preliminary aerodynamic and dynamic analysis is performed in order to assess the preliminary aerodynamic performance, the natural modes and the control sizing of the boxed wing configuration. The latter studies are not presented here as they are beyond the scope of the present work. The airfoil selected for the wing and the horizontal tail is the NACA 63-412 and the NACA 0008 for the vertical tails.

The main aircraft parameters are listed in 1: these are preliminary values for the present tentative design which can be changed in the future, with a detailed aircraft design.

2.2 ThrustPod overview

The TP technology is based on extractable thrusters that are able to generate the necessary vertical force for vertical take-off and landing. The thrusters are ducted fan or propellers driven by electric motors and arranged in a matrix shape with single or multiple layers. Even though there are several possible electric motors, the present work
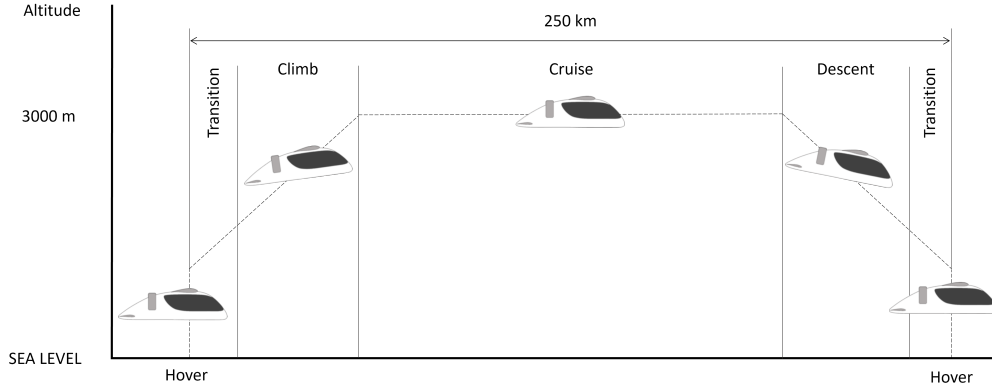
Figure 1: Mission of the urban air vehicle

Item	symbol	Unit measure	Value
Max fuselage length	l_f	m	8
Max fuselage width	w_f	m	1.5
Max fuselage height	h_f	m	2.0
Minimum TP height for a single layer	h_{TP}	m	0.25
Max ducted fan diameter	D_j	m	1.2
Max allowable power	P_{max}	kW	200
Stall velocity (without high lift)	V_s	km/h(m/s)	120 (33.3)

Table 1: Aircraft design constraints

considers off-the-shelf brushless permanent magnet ones. The power to mass ratio $5\,\mathrm{kW/kg}$ is assumed according to a linear regression obtained using available motors [2]. The same approach lead to define the controller board weight of $0.045\,\mathrm{kg/kW}$ obtained using available motors [2]. The propeller weight is calculated as proposed in [12].

As the TP is only intended for the hovering phases, additional thrusters are required for the climb, cruise and descent phases.
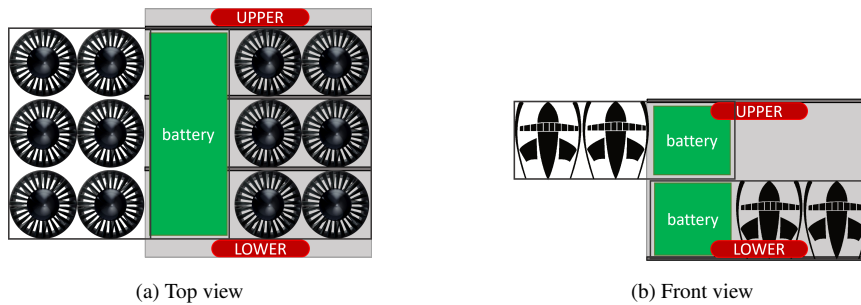

(a) Top view

(b) Front view

Figure 2: Top and lateral view of a possibile schematic arrangement of thrusters and battery inside the ThrustPod.

The Figure 2a illustrates an example of the two columns of three rows of thrusters, whereas the Figure 2b shows two layers of thrusters. The actuation system of Figure 2 is schematic and can be designed to achieve the required operations and requirements. Actuators work to extract and retract the thrusters that can slide on suitable rails and, therefore, very limited power is required. It is worth underlining that the space between the ducted fans can be used to store part of the energy needed for the aircraft mission.

At the present stage of the project, the aircraft is expected to have extractable skid, or legs, for static operations.

The TP is conceived to convert the modern fixed-wing aircraft to operate in the scenario of urban air mobility where the vertical take-off and landing capabilities are required. The main purpose is to exploit the advantages of a fixed thrust vehicle (e.g. multi-rotors) with the benefit of fixed-wing solutions to achieve long range performance. In order to achieve the latter objective, the basic idea is to avoid tilting thrusters or surfaces with the aim to split

the rotary wing and fixed-wing phase for independent optimisations. It is clear that the TP can be used to design an innovative urban air vehicle in order to optimise aerodynamics and the weight distribution. In fact, the present work deals with the preliminary design process of a full electric urban air vehicle based on the TP.

3 Integrated design approach

The TP design is connected to the aircraft design, and mainly to the fuselage design. In fact, increasing the TP's rows would increase the fuselage length. If the increase of propeller area would reduce the required power to generate the same vertical thrust, the longer fuselage would introduce higher structural weight and higher fuselage drag with a penalisation of the power required for the fixed wing phases. From the latter example, it is clear that a compromise between the maximum take-off mass (MTOM) and the design of the TP is necessary. The TP's independent variables are: 1) the fuselage length (that defines the number of possible rows) $l_f \in [4 - 8\,\mathrm{m}]$; 2) propeller diameter $D_j \in [0.3 - 1.2\,\mathrm{m}]$; 3) number of propellers $n_p \in [4, 150]$; 4) number of layers $n_l \in [1, 3]$. In order to optimise the power required to motors [9], the ducted fan are not co axial. Only when $n_l > 2$ an interference-induced power factor $k_{ind} = P_{co-axial}/P_{isolated} = 1.3$ is assumed.
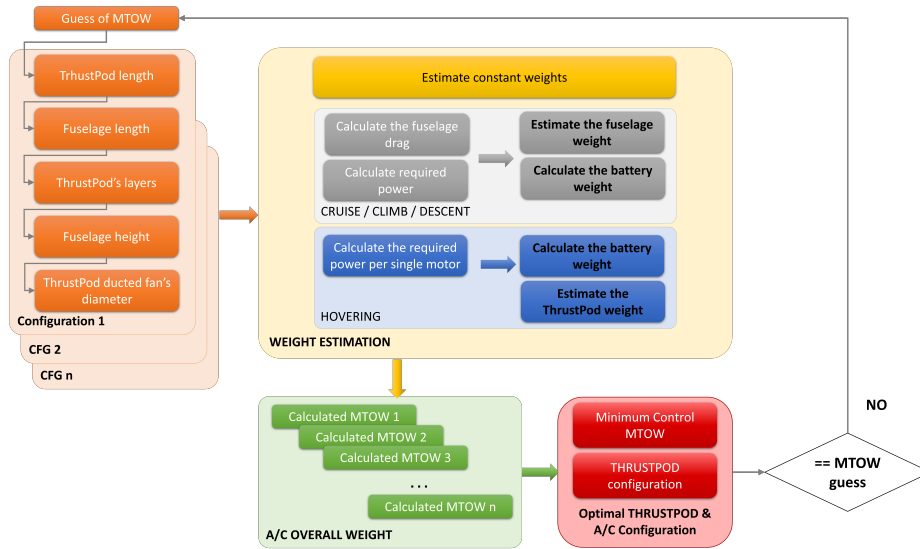

Figure 3: Design process of an urban air vehicle equipped with the ThrustPod.

The overall view of the design process proposed in the present work is in Figure 3. The starting point is the MTOM (or MTOW) guess. According to all possible combinations of the free parameters (l_f, D_j, n_p and n_l), several aircraft configurations are defined. Once the propeller diameter is set, it is clear that the number of ducted propellers n_j needs to be verified with respect to the available space (as function of the l_f). As far as the propeller arrangement is concerned, it is worth noting that two extraction chances are adopted: 1) symmetric full side extraction and 2) anti-symmetric saw-tooth extraction in order to optimise the available space on the TP.

For each one of the possible aircraft configurations, the power required for the hover flight by a single motor is estimated. Once the TP's motor power is estimated, the corresponding motor weight is evaluated considering the following contributions: i) motor; ii) propeller [12]; iii) controllers; iv) duct using a pseudo-density of $1\,\mathrm{kg/m}$ per unit of diameter; v) cable weight. Finally, the TP structure's weight is evaluated considering an extra pod under the fuselage [17] according to the current TP's size.

The overall weight of the TP is evaluated and the one that minimise the weight is not necessary the best that minimise the aircraft MTOW. The estimation of the aircraft weight is performed consdiering all significant contributions according to section 5.

Summing all contributions the aircraft weight W_{tot} is then calculated and compared with respect to the initial guess MTOW. The process is stopped if $|W_{tot} - \mathrm{MTOW}| = \mathrm{MTOW}_{thr}$, where the threshold $\mathrm{MTOM}_{thr} = 2\,\mathrm{kg}$. Otherwise the W_{tot} is used as first guess of the next iteration.

For a single layer, results of the TP weight calculation are reported in Figure 4. From Figure 4a, it can be noted that, even though only for the ducted propellers with $D_j = 0.2\,\mathrm{m}$ it is possible to achieve the global minima with 160 motors, the overall TP weight is higher for those configurations with D_j between $0.3\,\mathrm{m}$ and $0.6\,\mathrm{m}$. Whereas,

higher TP weights are calculated with larger diameters due to the limited available space. It is worth to underline that the configuration with $D_j = 0.9$ m does not lead to possible solution as the required power is higher than the P_{max}.

(a) Minimum of the ThrustPod weight

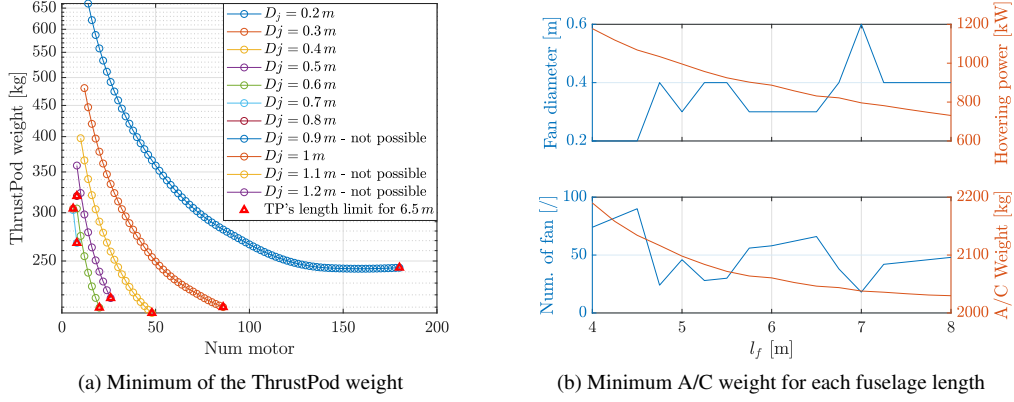(b) Minimum A/C weight for each fuselage length

Figure 4: Example of the outputs from a single iteration of the ThrustPod design process with a single layer.

The Figure 4b shows that for very short fuselage, $D_j = 0.2$ m minimises the overall aircraft weight using 74 motors. In this example, it can be noted that the minimum aircraft weight is obtained with the minimum TP weight using 48 units of $D_j = 0.4$ m.

4 Drag estimation

Zero-lift drag coeffient for climb, cruise and descent phases power and energy computation are needed, they are taken from [15]. The zero-lift drag for subsonic aircraft fuselage is:

$$C_{D0,f} = R_{wf} C_{Ff} \left[1 + \frac{60}{(l_f/d_f)^3} + 0.0025 \, (l_f/d_f) \right] \frac{S_{WET,f}}{S_w}$$
$$C_{Ff} = \frac{0.455}{\log Re_f^{2.58} (1 + 0.144 \, Ma^{0.58})} \tag{1}$$

where R_{wf} is the wing-fuselage interference factor, C_{Ff} the turbulent flat plate skin-friction coefficient of the fuselage, l_f/d_f the fuselage fitness ratio that is a function of the TP's height h_{TP}. Re_f is the fuselage Reynolds number and Ma the Mach number.

The zero-lift drag for subsonic aircraft wing is defined as:

$$C_{D0,w} = R_{wf} R_{LS} C_{Fw} \left[1 + L(t/c) + 100(t/c)^4 \right] \frac{S_{WET,w}}{S_w}$$
$$C_{Fw} = \frac{0.455}{\log Re_w^{2.58} (1 + 0.144 Ma^2)^{0.58}} \tag{2}$$

where R_{LS} is the lifting surface correction factor, C_{Fw} the turbulent flat plate friction coefficient of the wing, L the airfoil thickness location parameter, t/c the wing thickness ratio, $S_{WET,w}$ is the wetted wing area. Re_w is the wing Reynolds number.

The zero-lift drag for horizontal $C_{D0,ht}$ and vertical empennages $C_{D0,vt}$ (tails) have similar equation as Eq. (2), with their proper geometric parameters. The wing and empennages zero-lift drags can be summed together:

$$C_{D0,wTot} = C_{D0,w} + \frac{(C_{D0,ht} S_{ht} + 2 C_{D0,vt} S_{vt})}{S_w} \tag{3}$$

The vertical tail is accounted twice if the wing is boxed.

The sum of fuselage $C_{D0,f}$ and wing/empennages $C_{D0,wTot}$ results in the total C_{D0} zero-lift drag coefficient:

$$C_{D0} = C_{D0,f} + C_{D0,wTot} \tag{4}$$

5 Weight Estimation

5.1 Aircraft weights estimation

All the following estimated weights are expressed in lb_f measurement unit. Therefore, they are summed together to contribute to the aircraft total weight W_{AC}.

5.1.1 The Fuselage

Fuselage weight estimation is evaluated from [13]:

$$W_{FUS} = \left[0.052 \, S_{WET,f}^{1.086} \, (n_z W_O)^{0.177} \, l_{HT}^{-0.051} \left(\frac{l_{FS}}{d_{FS}} \right)^{-0.072} q^{0.241} \right] k_{f,c} \tag{5}$$

where $W_O = MTOM$ in lb_f unit measure, n_z is the ultimate load factor (1.5 x limit load factor), l_{FS} the fuselage structure length in ft, d_{FS} the fuselage structure depth in ft, q the dynamic pressure at cruise, n_z the ultimate load factor. $S_{WET,f}$ is the fuselage wetted area in ft^2 and it is defined as:

$$S_{WET,f} = 2l_f w_f + 2l_f h_f + 2w_f h_f \tag{6}$$

A fuselage factor $k_{f,c} = 0.75$ is taken into account in Eq. (5) for the composite material weight reduction [11].

5.1.2 Wing and horizontal tail

The weight equations for the wing are taken, [11], for light utility aircraft with performances up to $300 \, \mathrm{kn} \approx 556 \, \mathrm{km/h}$:

$$W_{wing} = 96.948 \left[\left(\frac{W_O \, n_z}{10^5} \right)^{0.65} \left(\frac{AR}{cos\Lambda_{1/4}} \right)^{0.57} \left(\frac{S_w}{100} \right)^{0.61} \left(\frac{1+\lambda}{2t/c} \right)^{0.36} \left(1 + \frac{V_e}{500} \right)^{0.5} \right]^{0.993} \tag{7}$$

where $AR = b_w^2/S_w$ the wing aspect-ratio, $\Lambda_{1/4}$ the wing quarter-chord sweep, S_w the wing area in ft^2, λ the wing taper ratio, t/c the maximum wing thickness ratio and V_e the cruise maximum speed at sea level equivalent airspeed in kn.

If a box-wing configuration is considered, the horizontal tail part (which is on fuselage bottom part) is treated as a wing and it has the same weight equation as Eq. (7), W_{HT}. Obviously with different parameters related to the new geometry, $S_{w,ht}$, AR_{ht}, $\Lambda_{1/4,ht}$, $(t/c)_{ht}$.

The weights of the main upper wing, Eq. (7), and the horizontal bottom part of the boxed-wing, can be summed together:

$$W_{wing,tot} = (W_{wing} + W_{HT}) \, k_{w,c} \tag{8}$$

where $k_{w,c} = 0.80$ is the wing reduction factor in mass for the usage of composite materials, [11].

5.1.3 The Vertical Tail

Vertical tail at the rear part of the fuselage has the following equation for weight estimation, [11]:

$$W_{VT} = 98.5 \left[\left(\frac{W_O \, N}{10^5} \right)^{0.87} \left(\frac{S_V}{100} \right)^{1.2} \left(\frac{b_V}{t_{VR}} \right)^{0.5} \right] k_{VT,c} \tag{9}$$

where S_V is the vertical tail area in ft^2, b_V the vertical tail span in ft, t_{VR} the vertical tail maximum root thickness in in. The mass reduction factor related to vertical tail, or empennage, composite material is then taken into account for the effective weight, it value $k_{VT,c} = 0.75$ is taken from [11].

5.1.4 The Avionics

The weight of the bare avionic equipment, W_{avio}, is evaluated accordig to statistical data [14] from the general aviation category. The installed avionic weight [11] is estimated as

$$W_{tron} = 2.117 \, (W_{avio})^{0.933} \tag{10}$$

5.1.5 The Furnishings

The furnishing weight in lb is estimated according to the formula proposed in [8]

$$W_{furn} = 32.03 n_{pax} + 54.99 \tag{11}$$

where the constant value is related to the pilot.

5.1.6 The Air Conditioning System

The air conditioning system's weight is evaluated from [14] as $W_{aircon} = 32.8 \, \text{kg}$

5.1.7 Flight Controls

Different weight estimation solutions are taken into account depending on the presence or not of a human pilot on board of the eVTOL aircraft. If the pilot is present, [13]

$$W_{fcs} = 0.053 \, l_{FS}^{1.536} \, b_w^{0.371} \left(n_z W_O \times 10^{-4} \right)^{0.80} \tag{12}$$

5.1.8 Electrical System

Weight estimation of electrical system is, [11]:

$$W_{electr} = 426 \left(\frac{W_{tron}}{1000} \right)^{0.51} \tag{13}$$

where W_{tron} is the avionics electric equipment of Eq. (10).

5.1.9 Miscellaneous

The miscellaneous weihgt formula proposed in [8] lead to estimations close to zero. The mean value $W_{misc} = 13.0 \, \text{kg}$ from [14] is considered.

5.1.10 Cruise Motors and Installation

The sizing process of the cruise motors is carried out with the objective to minimise the mass (motor and batteries) during the climb phase. Several rate of climbs and numbers of propellers are considered and the best trade-off is found with two ducted propellers with $1 \, \text{m}$ diameter to be installed on the aft part of the fuselage. The continuous installed power for the fixed-wing phases is $300 \, \text{kW}$ even though only the $33 \, \%$ is used during the cruise phase.

A prediction of motor (piston engine) installation weight can be considered for conservative reasons [14]. The predicted value is $W_{eng,inst} = 78.6 \, \text{kg}$.

5.1.11 The Landing Gear

The landing gear is considered retractable to reduce the aerodynamic drag. In order to estiamte the landing gear weight by a statistical point of view [8], in the present work it is assumed to have three (3) retractable legs (or skid) with a strut $l_{LG} = 0.4 \, \text{m}$ and an ultimate landing load factor $n_{Z,LG} = 2$. The weight is estimated as

$$W_{LG} = 3 \left[0.125 \left(n_{Z,LG} MTOM \right)^{0.566} \left(l_{LG}/12 \right)^{0.845} \right] \tag{14}$$

where MTOM is expressed in lb and l_{LG} in inches and the formula is related to nose landing gears.

5.2 Propulsive and energy storage system weight estimation

A general power system scheme for the aircraft is presented in 5, with direction of the input/output electrical and mechanical power. Additional components are connected to auxiliary battery (commonly $12 - 28 \, \text{V}$), but they are not shown in the scheme. This is architecture is very similar to automotive one, since there are common features. The following main components are connected to the ThrustPod system: i) AC Charger and AC/DC converter; ii) Power distribution unit (PDU); iii) Battery pack and management system; iv) Inverter; v) Electric motors and thruster modules; vi) Energy generator (alternator).
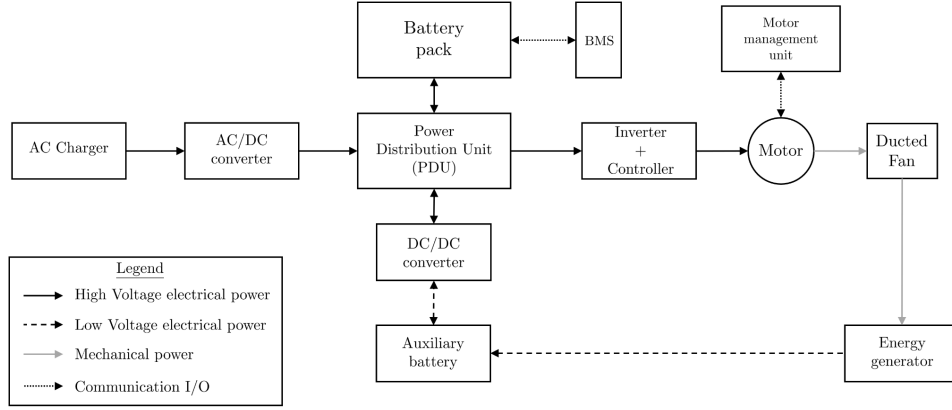
Figure 5: Power system scheme (simplified for one motor)

5.2.1 Efficiency evaluation

In this section some preliminary assumptions about efficiencies used in the present work are reported. The efficiency analysis is beyond the scope of the present work and its refinement could bring more accurate estimation for the proposed eVTOL design process based on the TP. Ducted propellers and related electronics are considered to evaluate the aircraft weight.

The efficiency chain for the fixed-wing phases is defined as

$$\eta_{cr} = \eta_B \eta_C \eta_M \eta_F \eta_D \eta_P =$$
$$= \frac{\text{power to controller}}{\text{power from the battery}} \frac{\text{power to motor}}{\text{power from controller}} \frac{\text{power to shaft}}{\text{power to motor}} \frac{\text{power to flow}}{\text{power from shaft}} \frac{\text{power to jet}}{\text{power from flow}} \frac{\text{power to aircraft}}{\text{power from jet}} \quad (15)$$

and the efficiency chain for the hover phases is defined as $\eta_h = \eta_B \eta_C \eta_M \eta_F \eta_D$.

The power required during the several phases are calculated as

$$P_h = \frac{P_{0,h}}{\eta_h}$$
$$P_{cr} = \frac{P_{0,cr}}{\eta_{cr}} \quad (16)$$

It is considered $\eta_B = 0.98$ during the cruise and $\eta_B = 0.80$ during the over phase due to the reduced efficiency at high discharge rates [10]. The efficiency of the duct takes into account the loss of the skin friction inside the duct. From [10] it is assumed a value of $\eta_D = 0.96$. Considering the chance to have independent phases (rotary and fixed wing), the motor can work around the project point. The efficiency of the motor is assumed from [1] as $\eta_M = 0.95$. The power electronics, the propeller and the propulsive efficiency are assumed from [10] as $\eta_C = 0.98$ and $\eta_F = 0.88$, $\eta_P = 0.95$. The maximum and minimum state of charge are $SOC_{max} = 1$ and $SOC_{min} = 0.1$ respectively.

Even though several advanced batteries are under study [19, 7], in the present work the energy density is assumed as $C_b = 0.320 \, \text{kW/kg}$ as in [10].

5.2.2 Hover

The following equations are required to compute the power for hover operations, which can be taken from [10] and [16]. Then the required energy and the mass of the batteries can be computed.

Total hovering time is set to $t_h = 4 \, \text{min}$ and, considering ducted propellers, the required power P_{h0} can be calculated as

$$P_{h,0} = \frac{0.5 \, T_{h0}^{3/2}}{\sqrt{\rho_h n_j A_{j,h}}} \quad (17)$$

where $T_{h,0} = $ MTOW, $\rho_h = 0.9091\,\mathrm{kg/m^3}$ evaluated at $z_h = 3000\,\mathrm{m}$ altitude, n_j the number of motors and $A_{j,h} = \pi\,(d_j/2)^2$ the area of ducted fans, with the fan diameter d_j. Finally $T_{h,0}$ is the lift force at least to equal the gravitational force downward $MTOW$, with $MTOW$ the maximum take-off weight of the aircraft and $g = 9.81\,\mathrm{m/s}$.

An additional force, and consequently power is added to P_{h0} to win aerodynamic resistance during vertical flight. The power P_{h1} can be computed as:

$$P_{h1} = D_{h1}V_h \tag{18}$$

where $D_{h1} = 0.5\rho v_h^2 S_w C_{D,h}$ and $C_{D,h} = 1$, for conservative reasons and $V_h = 5\,\mathrm{m/s}$ is the vertical speed. As $P_{h0} >> P_{h1}$, the required hovering energy is estimated as:

$$E_h = \frac{P_{h0}}{\eta_h \eta_{batt} t_h} \tag{19}$$

And the total mass for the hover is the combination of one for the battery $W_{h,b}$ and for the hover motors $W_{h,m}$:

$$W_{h,b} = \frac{E_h}{C_b} \tag{20}$$
$$W_{h,m} = n_j M_m$$

where C_b is the gravimetric energy of the selected battery, and M_m is the mass of the motors. It is worth noting that no global minimum can be found with Eq. (17), since both input variables n_j and d_j are inversely proportional to P_h, but as monotonic functions. Hence some constraints must be considered, as done with geometric optimization presented in section 3.

5.2.3 Climb

For the climb phase the required input parameters are: i) the climb gradient is γ_{cl}; ii) the true airspeed V_{cl}; iii) the vertical distance h_{cl}. The aerodynamic coefficients are:

$$C_{L,cl} = \frac{2\mathrm{MTOW}}{\rho\,S_w\,V S_{cl}} \cos\gamma_{cl}$$
$$C_{D,cl} = C_{D0} + \frac{C_{L,cl}^2}{\pi\,AR\,e\,K_{pr}} \tag{21}$$

where γ_{cl} is evaluated as described in section 5.1.10, C_{D0} is calculated according to section 4, e is the Oswald efficiency number and K_{pr} the Prandtl number. The required mass for the battery can be found as:

$$W_{cl,b} = \frac{E_{cl}}{C_b} \tag{22}$$

where $E_{cl} = \frac{P_{cl,0}}{t_{cl}\eta_{cr}}$, $\quad t_{cl} = \frac{h_{cl}}{v_{cl}\sin\gamma_{cl}}$, $P_{cl,0} = D_{cl}V_{cl}$ and $D_{cl} = 0.5\rho V_{cl}^2 S_w C_{D,cl} + MTOW g \cos\gamma_{cl}$. The distance covered during the climb phase is not negligible and is calculated as $d_{cl} = t_{cl}V_{cl}\cos\gamma_{cl}$.

5.2.4 Cruise

The cruise range can be estiamted as $d_{cr} = d_{max} - 2d_{cl}$ assuming that during the descent phase is flown the same horizontal distance druing the climb phase. The cruise speed is set to $V_{cr} = d_{cr}/1$ km/h. Coefficients of Eq. (21) can be rewritten for the cruise phase considering V_{cr} and a null rate of climb: $C_{L,cr} = \frac{2\mathrm{MTOW}}{\rho\,S_w\,V_{cr}}$ and $C_{D0} + \frac{C_{L,cr}^2}{\pi\,AR\,e\,K_{pr}}$

The battery weight required is:

$$W_{cr,b} = \frac{E_{cr}}{C_b} \tag{23}$$

where $E_{cr} = \frac{P_{cr,0}}{\eta_{cr}t_{cr}}$, $\quad t_{cr} = \frac{d_{cr}}{V_{cr}}$, $P_{cr,0} = D_{cr}V_{cr}$, $D_{cr} = 0.5\rho V_{cr}^2 S_w C_{D,cr}$. The motors are the same both for climb and cruise pahases and, therefore, $W_{cr,m} = W_{cl,m} = n_{cr,m}W_m$.

5.2.5 Descent, Spare

The descent phase is conservatively considered to be performed using the 20% of cruising power for the same time of the climb duration t_{cl} ($t_{de} = t_{cl}$). Therefore, the corresponding battery weight $W_{de,b} = \frac{E_{de}}{C_b}$ where $E_{de} = \frac{P_{cr,0}}{\eta_{cr}t_{cr}}$ and $P_{de,0} = 20\%P_{cr,0}$.

5.2.6 Transition phases

Considering the independent phases, the transition phases are limited to few seconds to accelerate the aircraft from the hovering phase to the stall speed. For the latter reason, the transition phases are not considered in the proposed design process.

5.3 Aicraft mass breakdown

Final aircraft mass can be computed as the sum of the partial masses shown in the previous sections:

$$W_{tot} = W_{h,b} + W_{h,m} + W_{cl,b} + W_{cr,b} + W_{cr,m} + W_{AC} + W_{pay} + W_{TP,frame}. \tag{24}$$

W_{pay} is the payload weight required for the passengers and pilot, the $W_{TP,frame}$ is the weight accounting for the TP's structural frame $W_{TP,frame}$.

6 Results

The results of the design process described in section 3 is reported in Table 2. The first three rows are the result of a single iteration starting from MTOM= 2100 kg as function of the TP's layer, n_l, in order to evaluate the differences between the possible best configurations. The proposed result comparison is important to highlight that for a fuselage less than 8 m for $5 + 1$ passengers, the best compromise is obtained with a double layer. In fact, it can be noted that the minimum weight is achieved adopting a TP with 36 ducted propellers driven by 16.8 kW electric motors. The exit velocity from the ducted propellers is about 170 km/h (47.2 m/s), whereas the power ratio to MTOM for hovering is higher than those available from statistical data [6]. This aspect is due to the less area used to generate the lifting force during the hovering phases. This apparent drawback is not a real issue as the hovering phases only represent 6 % of the entire mission. On the other side, the cruise power ratio to MTOM data is below than those available from statistical data [6] that represent a great advantage as the eVTOL is intended for sub-urban operations.

Another point of view of the same results is presented in Figure 6a. It can be noted that the minimum aircraft weight for the single layer is reached for fuselage length higher that the present limit. The optimal trade-off points for 2 and 3 layers are absolute minima conditions and therefore, a longer fuselage would lead to higher MTOM. The required diameters are between 0.3 m and 0.6 m. Whereas, larger diameters can be adopted for longer fuselages.

(a) Results of a single iteration of the design process

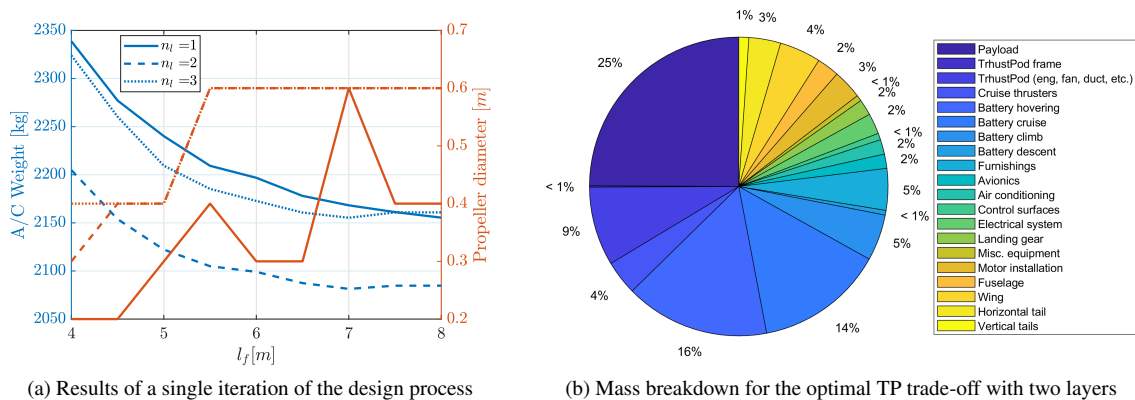(b) Mass breakdown for the optimal TP trade-off with two layers

Figure 6: Overview of the results from a single iteration of the proposed design process.

From the comparison of calculated and initial MTOM, it is clear that the optimisation problem is not converged and the first guess should be re-iterated. The optimal configuration is the last row of Table 2 with a final MTOM

of $2048\,\mathrm{kg}$. The corresponding mass breakdown is presented in Figure 6b with all contribution listed in section 5. From a first overview, the motor installation looks overestimated from [14] as its weight is higher then the entire fuselage structure. The overall battery weight is about the $25\,\%$ of the total MTOM. The TP weight is about $10\,\%$ of the total mass, whereas the thrusters' weight for the fixed-wing configuration is about $4\,\%$. The overall structure's weight (wing, fuselage and horizontal, vertical tails, landing gear and furnishings) is about $22\,\%$ where lighter composite structures are considered. The overall equipment mass budget (avionics, electric, control, air conditioning and miscellaneous) is about $8\,\%$.

n_l	Calculated MTOM	$l_f\,[\mathrm{m}]$	n_p	$D_j\,[\mathrm{m}]$	$P_j\,[\mathrm{kW}]$	$V_j\,[\mathrm{km/h}]$	$Hover\,[\mathrm{W/kg}]$	$Cruise\,[\mathrm{W/kg}]$
1	2155	7.9	48	0.4	16.4	221	365	95.9
2	2081	6.9	36	0.6	16.8	170	291	99.4
3	2155	6.9	54	0.6	11.9	139	298	96
2-*opt*	2048	6.9	36	0.6	16.2	168	285	94.4

Table 2: Aircraft and TrustPod tradeoff starting from MTOM= $2000\,\mathrm{kg}$ for several layers n_l and the converged solution 2-*opt* for two layers.

Even though the installed power would be less with the three layer configurations, the overall MTOM is similar to the double layer, whereas, the single layer leads to the highest calculated MTOM. The aircraft configuration is then chosen with two layers and a schematic view is reported in Figure 7.
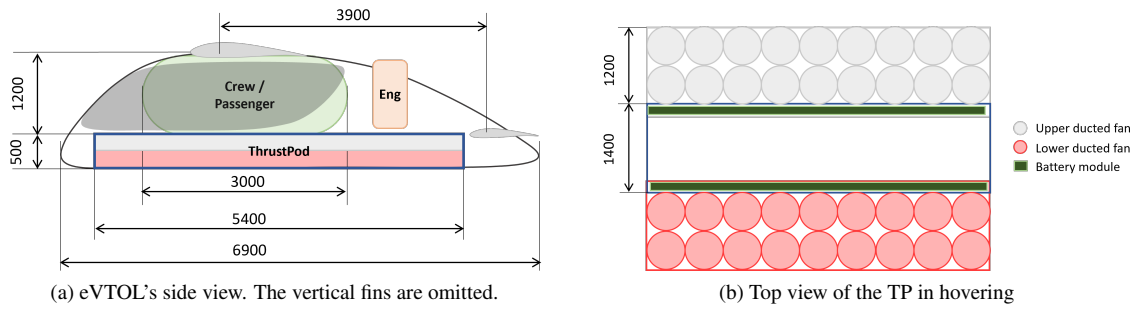

(a) eVTOL's side view. The vertical fins are omitted.

(b) Top view of the TP in hovering

Figure 7: Tradeoff of the aircraft and ThrustPod configuration with the minimum weight. All measures are in mm.

7 Conclusions

A novel solution named ThrustPod for urban air operations is proposed to reduce drag, weight, noise and actuated aircraft and propeller parts. As the hovering phase is very limited for sub-urban or regional UAM vehicles, the basic idea to optimise the cruise phase and, hence, working with a very efficient configuration by means of retracting independent thrusters that are only used for hovering phases. Although, the proposed solution penalises the available mass flow (or the propeller area) requiring higher power in hovering, the energy required for the hovering is limited if compared to the cruise phase. In fact, in the fixed-wing configuration, the aircraft has higher aerodynamic performances if compared to other eVTOL concepts that leads to a longer range. Even though the ThrustPod can be used to convert existing fixed-wing aircraft to urban operations, it can be used to design a novel eVTOL aircraft that contains the ThrustPod. An integrated environment for preliminary optimisation of the aircraft and the ThrustPod configuration is proposed. Following some preliminary assumptions, the fuselage length, the dimensions ducted propellers and the number of required driving motors are defined. The preliminary design suggests a promising configuration that is unique in the UAM scenario.

References

[1] Emrax innovative e-motors. https://emrax.com/e-motors/.

[2] MGM ComPro. https://www.mgm-compro.com/electric-motors/.

[3] World population prospects: Highlights, 2019.

[4] Ipcc, 2021: Summary for policymakers. in: Climate change 2021: The physical science basis. contribution of working group i to the sixth assessment report of the intergovernmental panel on climate change, 2021.

[5] Alessandro Bacchini and Enrico Cestino. Electric vtol configurations comparison. *Aerospace*, 6(3), 2019.

[6] Mehmet Efe Balli. Evtol aircraft conceptual design and optimization, 2020.

[7] Andrew Gibson, David Hall, Mark Waters, Philippe Masson, Benjamin Schiltgen, Trevor Foster, and Jonathan Keith. *The Potential and Challenge of TurboElectric Propulsion for Subsonic Transport Aircraft*.

[8] Snorri Gudmundsson. Chapter 6 - aircraft weight analysis. In Snorri Gudmundsson, editor, *General Aviation Aircraft Design*, pages 133–180. Butterworth-Heinemann, Boston, 2014.

[9] J.G. Leishman. *Principles of Helicopter Aerodynamics*. Cambridge Aerospace Series. Cambridge University Press, 2002.

[10] Patrick Nathen, Andreas Strohmayer, R. Miller, S. D. Grimshaw, and J. Taylor. Architectural performance assessment of an electric vertical take-off and landing (e-vtol) aircraft based on a ducted vectored thrust concept. 2021.

[11] Leland M. Nicolai and Grant E. Carichner. *Fundamentals of Aircraft and Airship Design, Volume 1 – Aircraft Design*. AIAA, 2010.

[12] R. M. Plencner, P. Senty, and T. J. Wickenheiser. Propeller performance and weight predictions appended to the navy/nasa engine program, 1983.

[13] D.P. Raymer. *Aircraft Design: A Conceptual Approach*. Number v. 1 in AIAA education series. American Institute of Aeronautics and Astronautics, 2006.

[14] J. Roskam. *Airplane Design*. Number pt. 5 in Airplane Design. DARcorporation, 1985.

[15] J. Roskam and C.T.E. Lan. *Airplane Aerodynamics and Performance*. Airplane design and analysis. Design, Analysis and Research Corporation, 1997.

[16] Renato Tognaccini. Lezioni di aerodinamica dell'ala rotante. 2008-2009.

[17] Egbert Torenbeek. *Fuselage design*, pages 61–95. Springer Netherlands, Dordrecht, 1982.

[18] UN General Assembly. Transforming our world: the 2030 agenda for sustainable development, 2015.

[19] Phil Whiffin. Batteries for aviation: Technology trajectories what is the future? 2019.